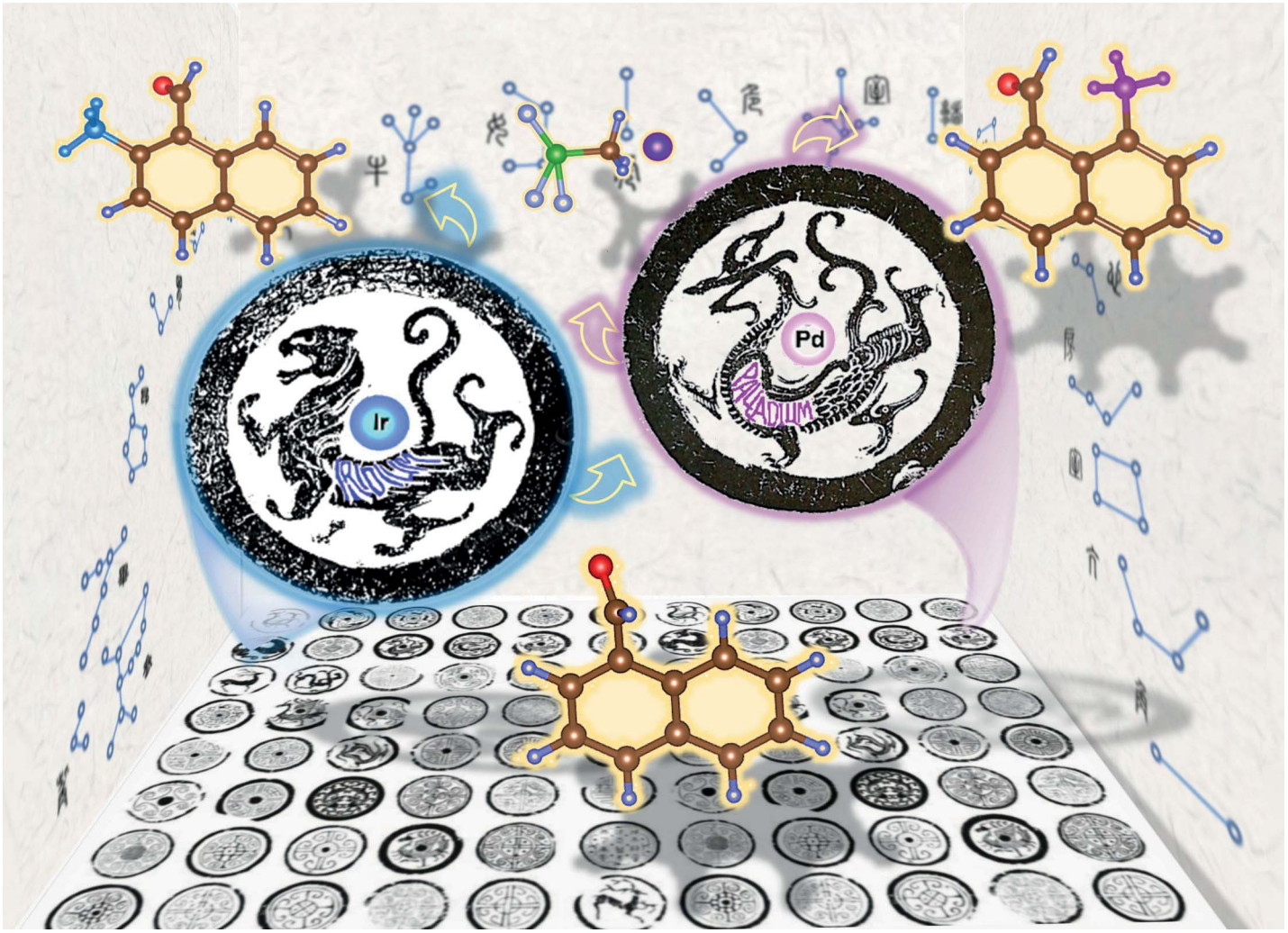

Professor Yinan Zhang and Professor Lihong Hu's laboratory, Jiangsu Key Laboratory for Functional Substances of Chinese Medicine, School of Pharmacy, Nanjing University of Chinese Medicine Nanjing, Jiangsu, China.

Overcoming *peri*- and *ortho*-selectivity in C–H methylation of 1-naphthaldehydes by a tunable transient ligand strategy

Assisted by dual metal/TDG catalysis, a regioselective *peri*- and *ortho*-C–H methylation of 1-naphthaldehyde has been realized with up to 96% yields, providing access to versatile multi-substituted naphthalene derivatives and natural products in simple steps. Experimental and computational studies verify the detailed mechanism of these conversions.

As featured in:

See Lihong Hu, Yinan Zhang *et al.*, *Chem. Sci.*, 2022, **13**, 2900.

ROYAL SOCIETY OF CHEMISTRY

rsc.li/chemical-science

Registered charity number: 207890

Chemical Science

ROYAL SOCIETY OF CHEMISTRY

EDGE ARTICLE

View Article Online
View Journal | View Issue

Cite this: *Chem. Sci.*, 2022, **13**, 2900

All publication charges for this article have been paid for by the Royal Society of Chemistry

Overcoming *peri*- and *ortho*-selectivity in C–H methylation of 1-naphthaldehydes by a tunable transient ligand strategy†

Yujian Mao,‡ Jing Jiang,‡ Dandan Yuan,‡ Xiuzhen Chen, Yanan Wang, Lihong Hu* and Yinan Zhang *

Received 26th October 2021
Accepted 3rd January 2022

DOI: 10.1039/d1sc05899a

rsc.li/chemical-science

Methyl groups widely exist in bioactive molecules, and site-specific methylation has become a valuable strategy for their structural functionalization. Aiming to introduce this smallest alkyl handle, a highly regioselective *peri*- and *ortho*-C–H methylation of 1-naphthaldehyde by using a transient ligand strategy has been developed. A series of methyl-substituted naphthalene frameworks have been prepared in moderate to excellent yields. Mechanistic studies demonstrate that *peri*-methylation is controlled by the higher electronic density of the *peri*-position of 1-naphthaldehyde as well as the formation of intermediary 5,6-fused bicyclic palladacycles, whereas experimental studies and theoretical calculations inferred that a 5-membered iridacycle at the *ortho*-position of 1-naphthaldehyde leads to energetically favorable *ortho*-methylation *via* an interconversion between the *peri*-iridacycle and *ortho*-iridacycle. Importantly, to demonstrate the synthetic utility of this method, we show that this strategy can serve as a platform for the synthesis of multi-substituted naphthalene-based bioactive molecules and natural products.

Introduction

The methylation strategy is of particular importance in accessing or optimizing bioactive molecules owing to the ubiquity of methyl groups in these pharmacological entities (Fig. 1A).[1] The development of site-specific methylation has attracted significant attention in the rapid construction and late-stage functionalization of complex structures.[2] Although a few regioselective methylation methods are well-developed for the transition metal (TM)-catalyzed *ortho*-C–H functionalization of benzene,[3] the precise site-selectivity control on polyaromatic ring systems (*e.g.* naphthalene) remains largely absent,[4] due to their possession of at least two proximal sites, the *peri*- and *ortho*-positions (Fig. 1B).

With the help of immobilized directing groups, such as picolinamides,[5] thioethers,[6] carboxylic derivatives,[7] amines,[8] hydrosilyls,[9] carbamates,[10] pyridyls,[11] phosphines,[12] and sulfonamides,[13]advances in *peri*- and *ortho*-C–H functionalization have been made, but most of these ligands have been restricted to C–H sp^2 functionalization (*e.g.* arylation, alkenylation, alkynylation, cyanation, *etc.*) and suffer from extra steps for installation and removal of directing groups (Fig. 1C). Although the transient directing group (TDG) strategy has been consequently devised to avoid using immobilized directing groups,[14] TDG promoted C–H alkylation remains extremely challenging. The only example, demonstrated by the Sorensen group, showed that the *in situ* formation of Schiff bases with benzaldehydes and orthanilic acids promoted *ortho*-C–H methylation and fluorination.[15] Our recent study has successfully extended the *peri*- and *ortho*-C–H oxygenation of polyaromatic rings.[16] Inspired by these discoveries, we envisioned that the precise site-selectivity control of proximal C–H alkylation of the naphthalene ring might be achieved *via* the incorporation of TDGs (Fig. 1D). To the best of our knowledge, we herein wish to disclose the first regioselective *peri*- and *ortho*-C–H methylation of 1-naphthaldehyde *via* TDG catalysis. The study not only features the site-specific metal incorporation and C–H cleavage, but also details mechanistic driving forces by providing consistent experimental and computational evidence.

Results and discussion

Peri-C–H methylation

Initially, we began our investigation by conducting *peri*-C–H methylation of 1-naphthaldehyde. Interestingly, the desired *peri*-C–H methylated product was detected in low yield after a 36 h reaction that used 10 mol% of $Pd(OAc)_2$ as the catalyst, 60 mol% of glycine (**TDG1**) as the TDG, 2.0 equivalents of AgOAc as the oxidant, 2.5 equivalents of potassium methyl trifluoroborate

Jiangsu Key Laboratory for Functional Substances of Chinese Medicine, School of Pharmacy, Nanjing University of Chinese Medicine Nanjing, Jiangsu, 210023, China. E-mail: yinanzhang@njucm.edu.cn; lhhu@njucm.edu.cn

† Electronic supplementary information (ESI) available: Experimental procedures, characterisation data, computational details, and copies of ^1H and ^{13}C NMR spectra for all compounds featured in this manuscript. See DOI: 10.1039/d1sc05899a

‡ These authors contributed equally.

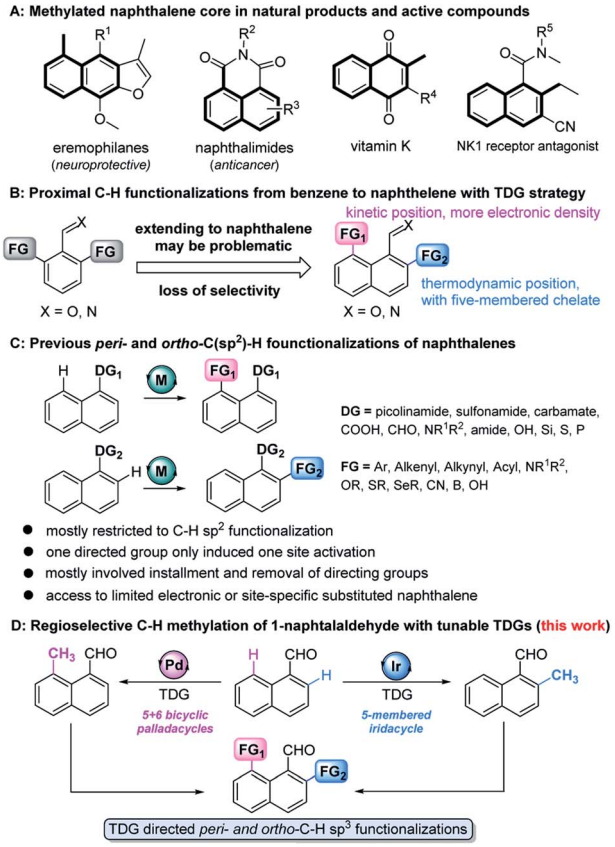

Fig. 1 (A) Methyl groups in natural products and bioactive molecules. (B) Selectivity from benzene to naphthalene. (C) *Peri*- and *ortho*-C–H functionalizations of naphthalene. (D) Regioselective C–H methylation of 1-naphthaldehydes with tunable TDGs.

as the methylating reagent, and acetic acid (0.2 M) as the solvent (Table S1†). Striving to improve the reaction efficiency, we examined numerous oxidants and found that $Cu(TFA)_2$-xH_2O (ref. 17) performed better than other oxidants. Previously reported F^+ oxidants failed to give the C–H methylation product at the *peri*-position.[15] Next, screening of basic additives showed that two equivalents of CsOAc gave a better yield (35%). Surprisingly, the addition of H_2O that facilitated the solubility of trifluoroborate salt improved the yield to 43%, and yet adopting soluble methylboronate $MeBF_3(Bu_4N)$ and other methylating reagents inhibited the yield (Tables S1 and S2†). The screening of solvents, for example, hexafluoroisopropanol (HFIP) further promoted the reaction yield to 48%, while only traces of *ortho*-product **3a** or bi-methylated product **4a** were detected. Subsequent optimization of TDG ligands demonstrated that the presence of L,X-type TDGs is critical to C–H methylation, probably because the *peri*-selectivity relied on the formation of bicyclic palladacycles (Table 1). Using carbonyl as the X-branch of the ligand (**TDG1, 7, 8**) preferably gave the *peri*-product, whereas reactions involving the use of sulfonic acid as the X-branch (**TDG2, 5**) and monodentate ligands (**TDG3, 6**) were biased towards the bi-methylated product. Meanwhile, extended L,X-TDGs (**TDG4, 5, 9**) triggered a higher ratio of Pd insertion at the *ortho*-position, since the bicyclic palladacycle

Table 1 Effects of TDGs on *peri*-C–H methylation of 1-naphthaldehyde[a,b]

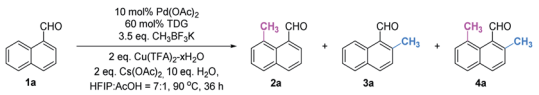

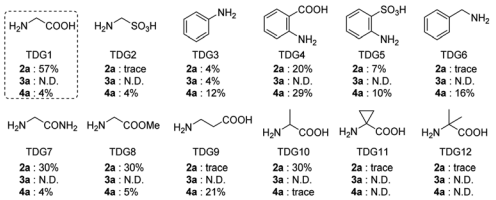

[a] Experiments were performed under the following reaction conditions: **1a** (0.3 mmol), CH_3BF_3K (1.05 mmol), $Pd(OAc)_2$ (10 mol%), TDG (60 mol%), $Cu(TFA)_2$-xH_2O (0.6 mmol), CsOAc (0.6 mmol), HFIP : AcOH = 7 : 1 (1.5 mL), H_2O (3.0 mmol), 90 °C, sealed tube, 36 h. [b] Yields were determined by ^1H NMR analysis of the crude reaction mixture using CH_2Br_2 as the internal standard.

with a 5,6-fused ring has the most favorable ring strain.[18] However, steric L,X-type TDGs (**TDG10–12**), which destabilized the conformation of bicyclic palladacycles, reduced the reactivity.

With the optimal reaction conditions in hand, we next explored the scope of *peri*-C–H methylation (Table 2). Various substituted 1-naphthaldehydes bearing electron-neutral, donating and withdrawing groups were smoothly methylated in uniformly moderate yields. Substrates with substituents in universal positions could provide the corresponding products.

Table 2 Scope of 1-naphthaldehyde for *peri*-C–H methylation[a,b]

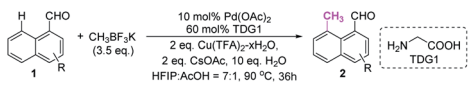

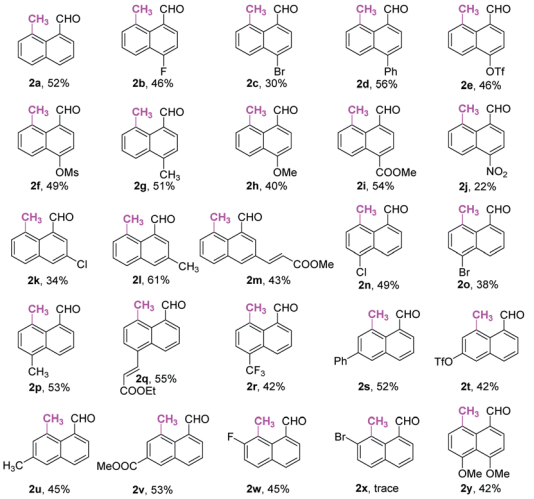

[a] Under the same conditions as in Table 1. [b] Isolated yields.

Gratifyingly, sulfonates (**2e**, **2f**, **2t**) and acrylates (**2m**, **2q**) were amenable with the reaction system. Previously prohibited substrates, such as those with formidable withdrawing and donating groups (**2j**, **2y**), also gave the desired products. The limitation of the method occurs only on the steric substitution at the 7-position (**2x**).

Ortho-C–H methylation

Although we have detected the existence of *ortho*-products (**TDG3**, Table 1) during the optimization of *peri*-C–H methylation, the yield with Pd catalyst is difficult to improve after futile efforts. The higher electron density at the *peri*-position allows the C–H activation to inevitably occur prior to the *ortho*-position. Inspired by previous studies,[19] we hypothesized that iridium may override the unnecessary activation at the *peri*-position. To our delight, the *ortho*-C–H methylated product was found dominantly when using $[Cp^*IrCl_2]_2$ and TDG3, although accompanied by a trace quantity of di-methylated **4a**. Extensive screening of solvents, oxidants, additives and methylating reagents resulted in no yield enhancement (Tables S3 and S4†), while thorough investigation of the TDGs implicated that simple anilines were superior to the L,X-type ligands (Tables 3 and S3†). Finally, we identified that *meta*-EWG containing TDGs (**TDG25, 28**) were the optimal ligands for *ortho*-C–H methylation.

With the optimized procedure in hand, we next explored the scope of *ortho*-C–H methylation. All the substituted 1-naphthaldehydes previously studied for *peri*-C–H methylation were revisited. It was found that not only all sorts of electron properties but also universal sites of substituted naphthaldehydes were well-tolerated to generate the expected *ortho*-products with excellent yields. Although substrates with steric hindrance and electron-donating substituents[19a] were found to inhibit the reactivity, 3-aminobenzonitrile (**TDG28**) dramatically promoted the reactivity of these steric (**1k**, **1l** and **1m**) and electron donating substrates (**1h** and **1y**). When the di-CN TDG group was used (**TDG29**), the yield of **3y** further increased to 71%, indicating that the electron-withdrawing TDG is favorable for *ortho*-C–H methylation. The poor convertion of *peri*-occupied substrates (**2a** and **1ab**) inspired our further study of mechanism.

Table 3 Scope of 1-naphthaldehyde for *ortho*-C–H methylation[a,b]

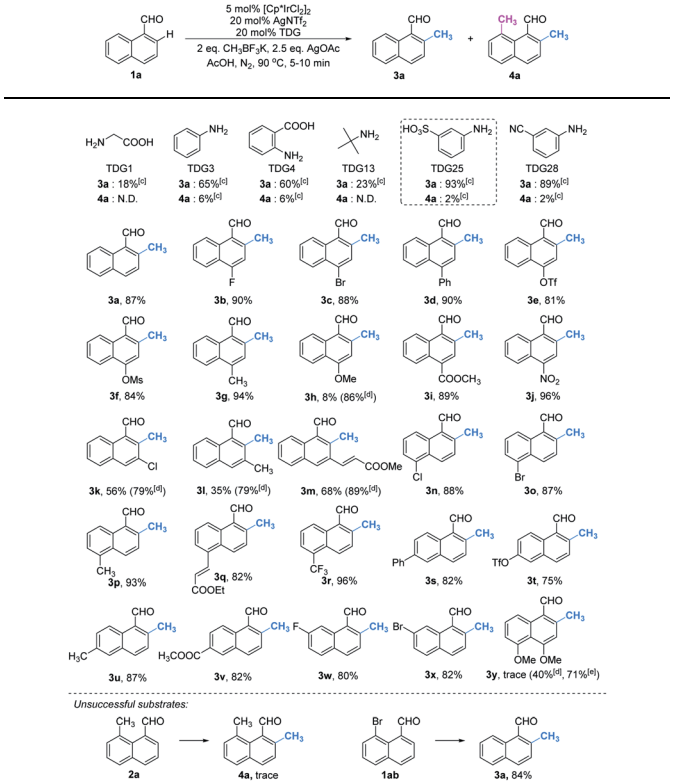

[a] Experiments were performed under the following reaction conditions: **1a** (0.3 mmol), CH_3BF_3K (0.6 mmol), $[Cp^*IrCl_2]_2$ (5 mol%), TDG (20 mol%), $AgNTf_2$ (0.06 mmol), AgOAc (0.75 mmol), AcOH (1.5 mL), 90 °C, N_2, sealed tube, 5–10 min. [b] Isolated yields. [c] Yields were determined by ^1H NMR analysis of the crude reaction mixture using CH_2Br_2 as the internal standard. [d] **TDG28** was used instead of **TDG25**. [e] **TDG29** was used instead of **TDG25**, 30 min.

Synthetic applications to naphthalene-based derivatives and natural products

Based on the above studies, we devoted our efforts to demonstrating the synthetic utility of this protocol. As shown in

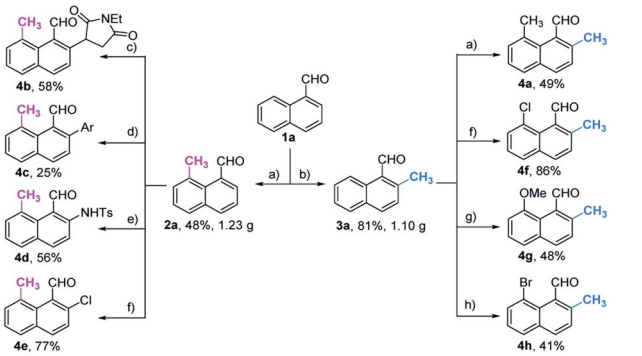

Scheme 1 Synthesis of diverse naphthaldehydes *via* sequential C–H functionalizations[a]. [a]Reaction conditions: (a) **1a** or **3a**, CH_3BF_3K (3.5 eq.), $Pd(OAc)_2$ (10 mol%), TDG (60 mol%), $Cu(TFA)_2$-xH_2O (2 eq.), CsOAc (2 eq.), HFIP : AcOH = 7 : 1, H_2O (10 eq.), 90 °C, sealed tube, 36 h. (b) **1a**, CH_3BF_3K (2 eq.), $[Cp^*IrCl_2]_2$ (5 mol%), TDG (20 mol%), $AgNTf_2$ (20 mol%), AgOAc (2.5 eq.), AcOH, 90 °C, N_2, sealed tube, 4 h. (c) **2a**, $[Ru(p\text{-cymene})Cl_2]_2$ (5 mol%), $AgSbF_6$ (20 mol%), 2-methyl-3-(trifluoromethyl)aniline (20 mol%), 4-chlorobenzoic acid (0.5 eq.), 1-ethyl-1*H*-pyrrole-2,5-dione (1.5 eq.), DCE : HFIP = 5 : 1, 60 °C, N_2, sealed tube, 36 h. (d) **2a**, $Pd(OAc)_2$ (10 mol%), methyl 4-iodobenzoate (2 eq.), 2-amino-2-methylpropanoic acid (40 mol%), AgTFA (1 eq.), HFIP : TFA = 9 : 1, 110 °C, sealed tube, 24 h. (e) **2a**, $[CpIrCl_2]_2$ (4 mol%), 3-trifluoromethylaniline (40 mol%), 4-methylbenzenesulfonyl azide (2 eq.), $AgPF_6$ (24 mol%), DCE, 100 °C, N_2, sealed tube, 36 h. (f) **2a** or **3a**, NCS (1.3 or 1.5 eq.), $Pd(OAc)_2$ (10 mol%), anthranilic acid (30 mol%), AgTFA (10 mol%), TFA (10 eq.), DCE, 60 °C, sealed tube, 24 h. (g) **3a**, $Pd(OAc)_2$ (10 mol%), $K_2S_2O_8$ (2 eq.), MeOH (20 eq.), 3-(trifluoromethyl) aniline (40 mol%), CH_2Cl_2, 60 °C, sealed tube, 36 h. (h) **3a**, NBS (1.5 eq.), $Pd(OAc)_2$ (10 mol%), 2-amino-4-nitrobenzoic acid (50 mol%), AgTFA (10 mol%), TfOH (50 mol%), DCE, 90 °C, sealed tube, 24 h.

Scheme 1, methylated products **2a** and **3a** can be obtained on gram scales with 48% and 81% yields respectively. Diverse disubstituted naphthalene derivatives were achieved *via* sequential C–H functionalization at the proximal positions of aldehydes with reactive groups, such as alkyl, aryl, halogen, sulfonamide, and alkoxy. Interestingly, 2,8-dimethyl-1-naphthaldehyde **4a** could be obtained if the methyl group was first introduced at the 2-position (Table 3) rather than at the 8-position (Scheme 1).

In our further attempt to demonstrate the synthetic utility, several bioactive compounds[20] that bear alkyl-substituted naphthalene frameworks have been obtained efficiently (Scheme 2). For example, the preparation of nordehydrocacalohastine (**11**), an antimicrobial eremophilane sesquiterpene first isolated from *Cacalia* and *Senecio* plants,[21] started from commercially available naphthol **5**. Naphthaldehyde **7** was readily acquired by the Rieche reaction of compound **6** with high regioselectivity. After protection of the phenol group with α-bromoacetone, *peri*-methylation was successfully carried out to deliver the key intermediate **9** in a yield commensurate with the above standard conditions. Subsequent deformylation and cyclization accomplished the synthesis of the natural product in a total of 6 steps. Impressively, the employment of our methylation method saves 6 steps and improves the total yield 4.5-fold (11.7% *vs.* 2.6%) compared with the previously reported route.[22] Meanwhile, gram methylation of 3-bromo-naphthaldehyde gave the *ortho*-methylated naphthaldehyde **13** in 80% yield. Next, treatment with the standard Bayer–Villiger reaction and oxidation smoothly produced the key precursor quinone **15**, providing an alternative route to vitamin K.[23] The final example was illustrated by the exchange of substitution on 4-fluoronaphthaldehyde. *Peri*-methylation and removal of the formyl group gave **16**. Oxidation of the existing methyl group to another aldehyde **17** achieved *ortho*-methylation to form a rare 2-methyl-5-fluoronaphthaldehyde in 82% yield. These serial conversions highlighted the unique merit of our method in the preparation of naphthalene-based natural products and bioactive derivatives.

Mechanistic studies

To gain mechanistic insight into this reaction, a set of control experiments were carried out. In the absence of a catalyst or a TDG group, little product was detected under the standard conditions. The addition of a radical scavenger cannot quench the methylated products (Scheme 3, A1 and B1), indicating a non-radical process. Slightly reversible H/D exchange occurred at the *peri*-C–H position in the presence of $Pd(OAc)_2$, while addition of glycine increased the ratio of the deuterated product. This observation verified the promotive effect of the TDG (Scheme 3, A2). Equivalent mixtures of EDG (**1h**) and EWG (**1j**) substrates under standard conditions of *peri*-methylation resulted in a large ratio of product **2h**, illustrating that the electron-rich naphthaldehyde reacted faster than the electron-deficient one (Scheme 3, A3), while *ortho*-methylation had a much faster rate with electron-withdrawing substitutions (Scheme 3, B3). The stable palladacycle **19** was successfully captured by the pyridine ligand and could be further converted to the *peri*-methylated product **2a** (Scheme 3, A4). Moreover, addition of product **2a** was found to inhibit *peri*-methylation of **1a** (Scheme S1†), which may explain the moderate yields of this conversion.

However, treatment of **1a** with $[Cp^*IrCl_2]_2$ in AcOD delivered deuterated products at both *peri*- and *ortho*-positions. The higher D-ratio at the *peri*-position with standard and extended

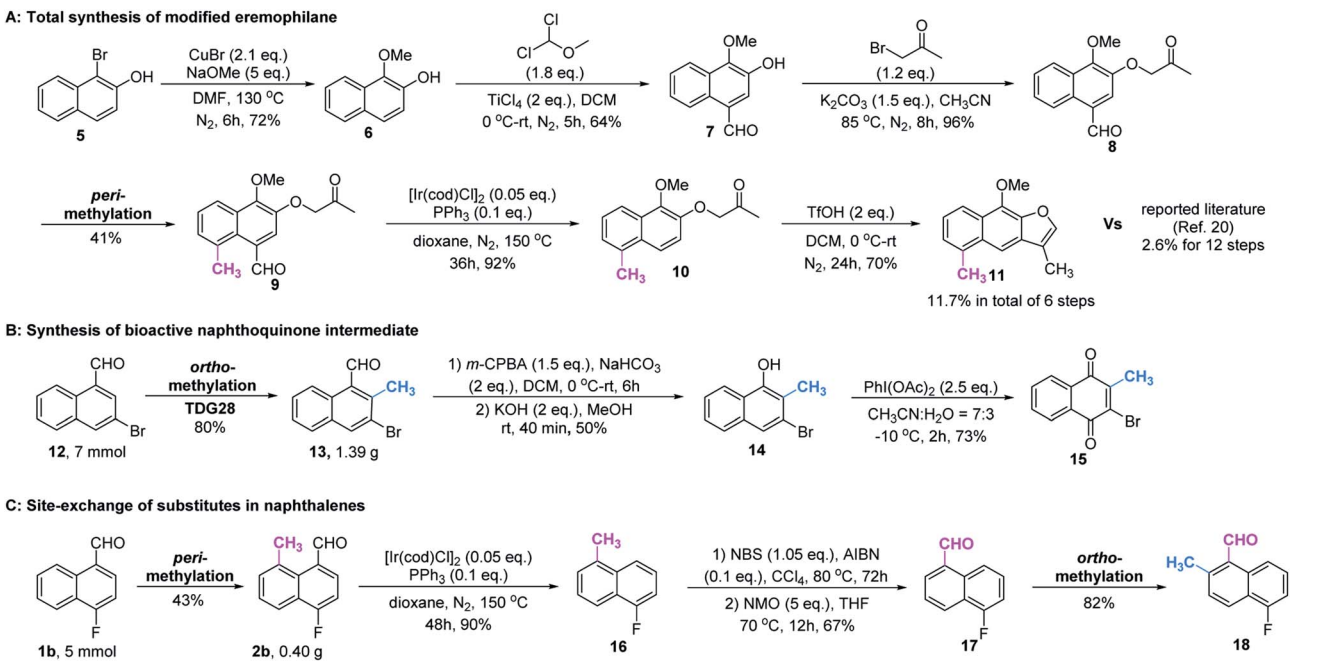

Scheme 2 Synthetic transformation of regioselective *peri*- and *ortho*-C–H methylation.

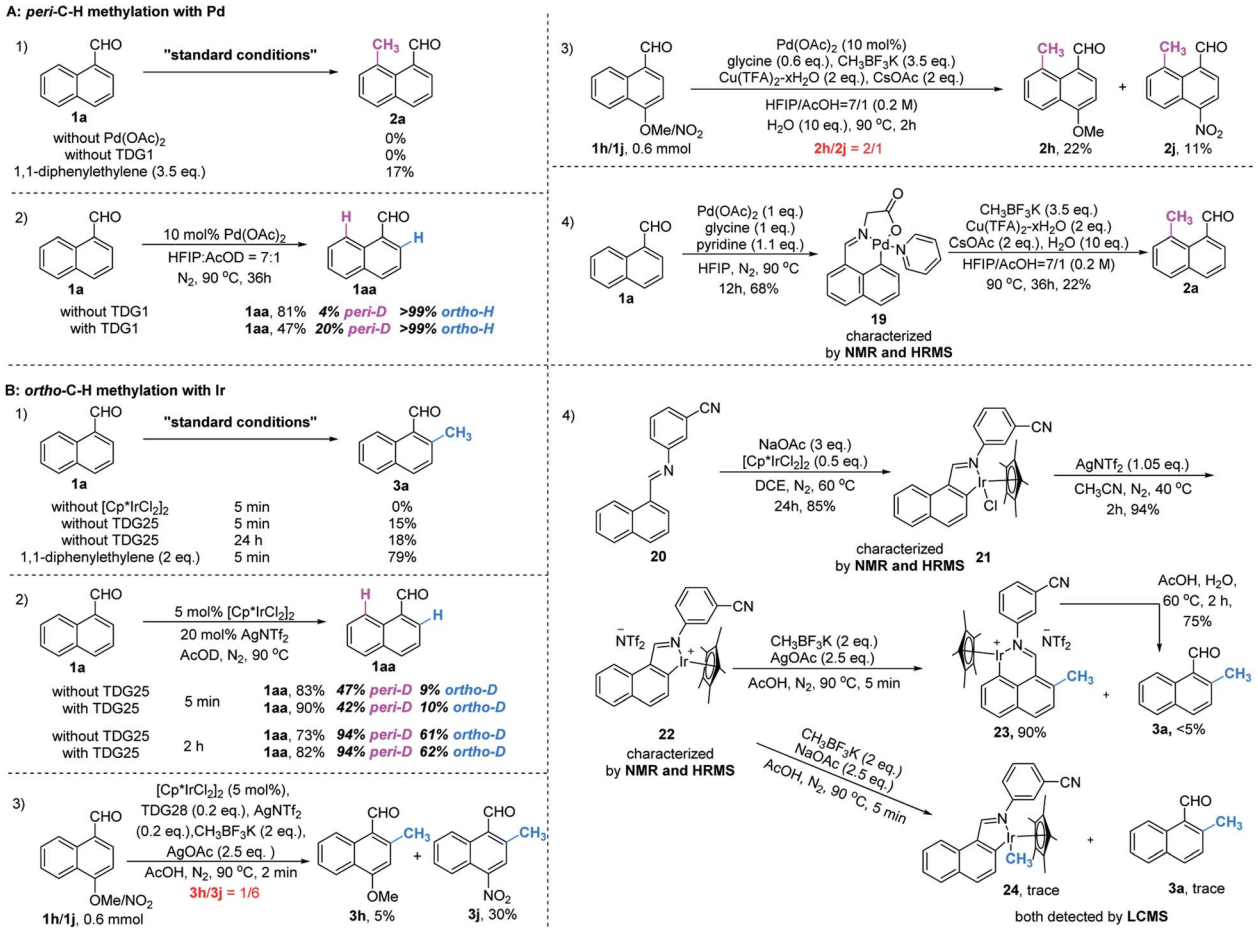

Scheme 3 Mechanistic studies.

reaction times consistently showed that the *peri*-position is more likely to have the metal inserted due to its higher electronic density than the *ortho*-position,[16] and even the introduction of **TDG25** had no influence on this outcome (Scheme 3, B2). Although the rate of *peri*-metallation may be superior to the rate of methylation at the *ortho*-position in the C–H metal insertion step, it was found that the *peri*-iridacycle was readily hydrolysed, which also explains the higher yield of the deuterated product at this position. In contrast, resistance to *ortho*-hydrolysis resulted in the capture of iridacycle **21** and its NTf_2 ligand exchanger **22** (Scheme 3, B5). Treatment with CH_3BF_3K produced iridacycle **24** and the desired *ortho*-methylated product **3a** in the absence of an oxidant. However, in the presence of an oxidant, *ortho*-iridacycle **22** was converted to *peri*-iridacycle **23** when the *ortho*-position was occupied by the methyl group. And *peri*-iridacycle **23** was readily acid hydrolyzed to product **3a** rather than successive methylation at the *peri*-position. Notably, the observations that *ortho*-iridacycle **22** was resistant to acid hydrolysis and *peri*-blocked substrates (**3z** and **4a**, Table 3) diminished the *ortho*-productivity further corroborated the fact that the reactivity of and interconversion between these iridacycles together controlled the *ortho*-selectivity (Scheme 3, B4). Additionally, the poor reactivity of simple benzaldehyde in our method showed that the methylation method had unique properties in the selective activation of the proximal C–H bonds of naphthaldehyde (Scheme S2†). Finally, determination of the kinetic isotope effect (KIE) of the C–H cleavage was carried out (Scheme S3†). The intermolecular KIE of **1a** and **1a-*peri*-D** was found at 0.99 (k_H/K_D), which indicated that the cleavage of the *peri*-C–H bond is not involved in the rate-determining step. Similarly, the KIE of the *ortho*-C–H bond was studied at a low temperature to slow the conversion for measurement. The intermolecular KIE of **1a** and **1a-*ortho*-D** is 1.30 (k_H/K_D), which suggested that the cleavage of the *ortho*-C–H bond may not be involved in the rate-determining step.

Computational studies

Since the control experiment suggested that the *peri*-palladacycle directed the following methylation, the mechanism for the palladium-catalyzed *peri*-C–H activation process was thus investigated using M06-2X DFT calculations. As shown in Fig. 2A, the transition state of **TS2** possessed a lower energy barrier ($\Delta G^{\ddagger}$ = 11.9 kcal mol^{-1}) at the *peri*-position, in comparison with the transition state **TS1** guiding the *ortho*-C–H insertion ($\Delta G^{\ddagger}$ = 16.5 kcal mol^{-1}). At the same time, the lower energy level of *peri*-intermediate **Int3** over **Int2** also indicated that the higher electron density at the *peri*-position of 1-naphthaldehyde controlled the selectivity. In order to obtain details

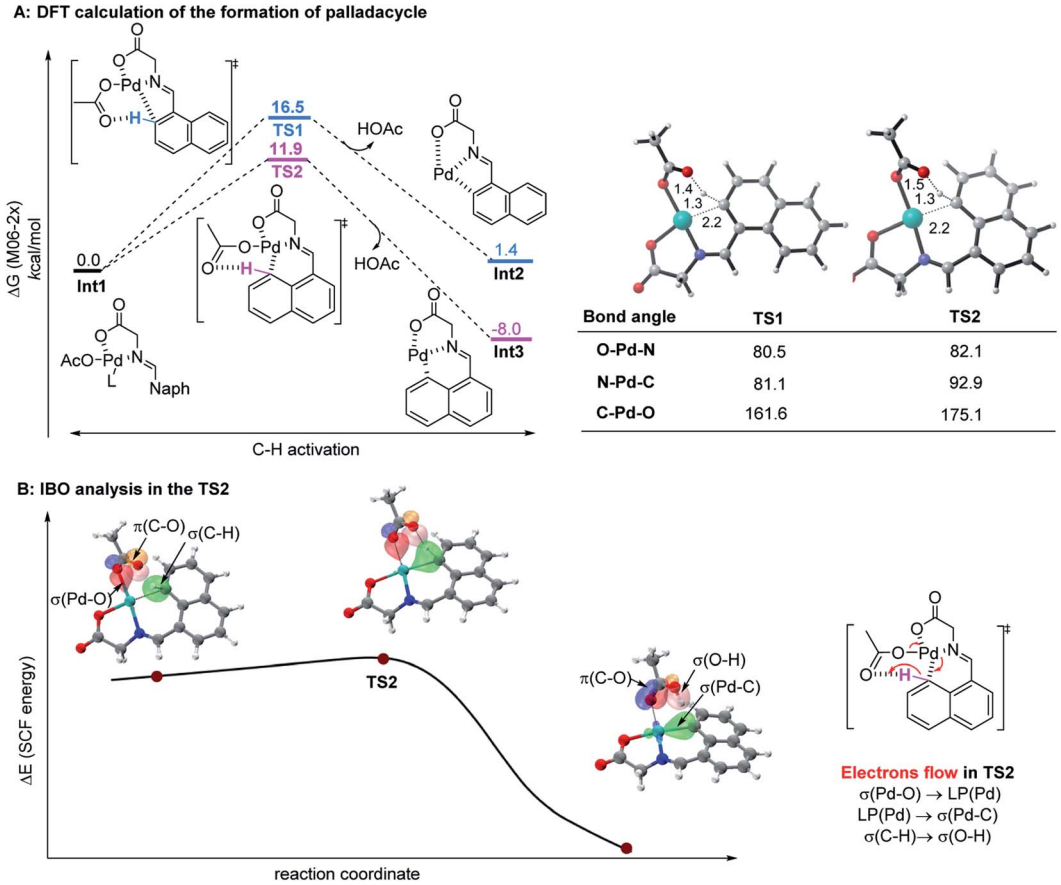

Fig. 2 (A) The calculated reaction energy profile of palladacycle complex formation steps. (B) IBO analysis of the palladium-assisted *peri*-C–H activation of TS2.

on the actual electron flow in the conversion, an intrinsic bond orbital (IBO) analysis was performed (Fig. 2B).[24] In the TS2 structure, the electrons in the σ-orbital [aromatic C–H] interact with the π*-orbital [C═O] of acetate to abstract a proton. The electrons of [σ(Pd–O)] become a lone pair [LP(Pd)] of the palladium complex, and at the same time, the electrons in the 4d-orbital of palladium [LP(Pd)] form a new palladium–carbon σ-bond [σ(Pd–C)] in the palladacycle intermediate. The bond recombination occurs *via* a concerted mechanism.[25]

The mechanism of the *ortho*-C–H activation process with the iridium catalyst was also investigated following the experimental findings (Fig. 3A). As anticipated, starting from the relative zero point of the iridium-Schiff base complex, *peri*-metallation had a lower energy barrier of 3.5 kcal mol^{-1} than *ortho*-metallation. After C–H insertion, the *peri*-iridacycle was also found to be more stable than its *ortho*-counterpart **22.** Subsequent transmetallation with CH_3BF_3K flipped over the Gibbs energy, in which *ortho*-product **24** was exothermic by 7.4 kcal mol^{-1}, 11.1 kcal mol^{-1} higher than that of the process that yielded the *peri*-product. The addition of the Cl ligand to the intermediates **Int5** and **Int6** also reversed their stability, which was exactly validated by the isolation of iridacycle **21** rather than ***peri*-21.** In the intrinsic bond orbital (IBO) analysis, a similar pattern of electron flow to that of the palladacycle had been verified (Fig. 3B).

Previous findings prove that the energy barrier of reductive elimination is lowered at least by 15–30 kcal mol^{-1} by increasing the oxidation state of iridium from product-like Ir(III) to reactant-like Ir(V).[26] We postulated that oxidatively enhanced reductive elimination was also dominant in our *ortho*-methylation after iridium was oxidized to hypervalent species by the silver oxidant. As shown in Fig. 3C, active *ortho*-Ir(V) species **Int7** underwent reductive elimination and coupled the methyl group to the naphthalene ring releasing a large amount of energy (41.4 kcal mol^{-1}), in which the energy barrier of *ortho*-methylation was 14.2 kcal mol^{-1} (2.7 kcal mol^{-1} lower than that of the unfavorable *peri*-methylation). Next, the iridacycle rebounded to the *peri*-position to produce intermediate **23** as experimentally observed, by continuing to release 4.9 kcal mol^{-1} of energy. Overall computational calculations indicated by the energy profile of transient states were in complete agreement with experimental investigations and supported the regioselectivity.

Collectively, we proposed a plausible catalytic cycle that is believed to be different from previously reported Pd(II)/(IV)[15] and Ir(I)/(III)[19a] catalysis (Scheme 4). Starting from the formation of imine **A** or **E**, metal catalysts are incorporated into the activated C–H bond and afforded a 5,6-fused bicyclic or 6-membered ring at the *peri*-position. Insertion of CH_3BF_3K to the palladacycle induces subsequent reductive elimination to forge precursor **D**. For the iridacycle, hydrolysis and re-iridation promote the

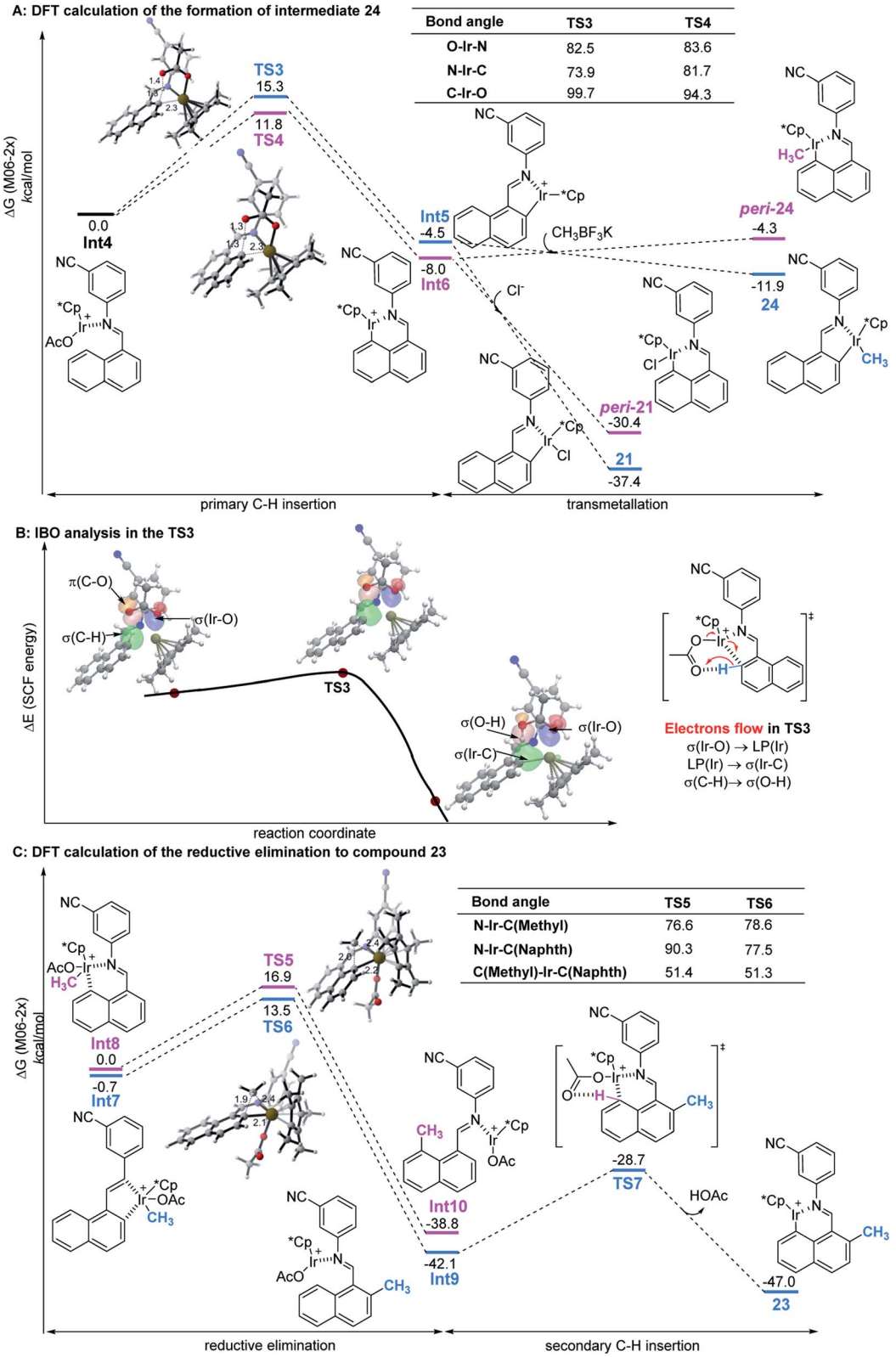

Fig. 3 (A) The calculated reaction energy profile of the formation of intermediate **24**. (B) IBO analysis of the iridium-assisted *ortho*-C–H activation of **TS3**. (C) The calculated reaction energy profile of the formation of product **23**.

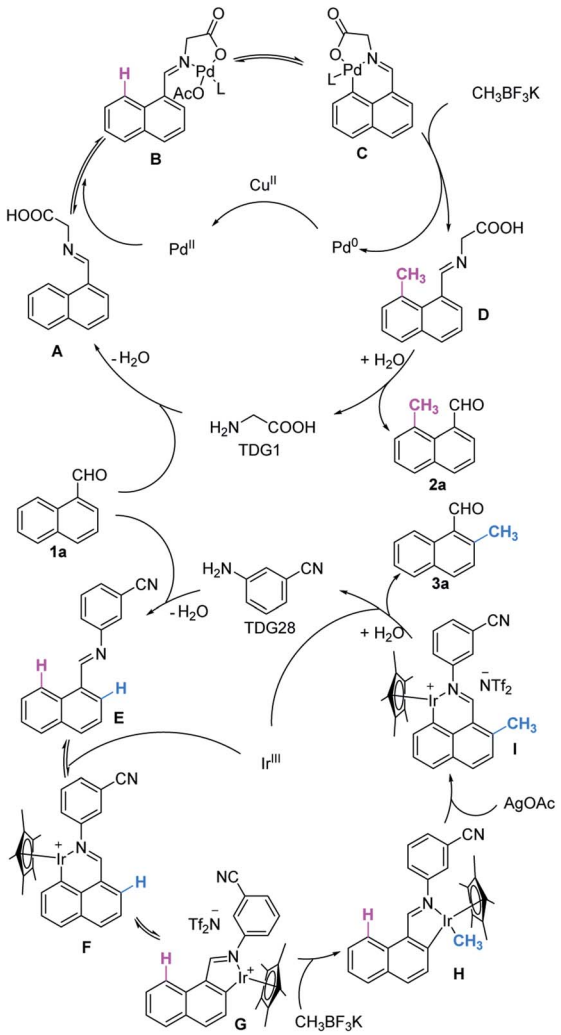

Scheme 4 Possible mechanistic pathway.

conversion of 6-membered ring **F** to 5-membered ring **G,** which is ready to perform transmetallation with a methylated reagent. After the oxidatively induced reductive elimination of iridacycle **H**, *ortho*-methylation brings about another *peri*-iridation to form intermediate **I** which is reactively inert to methylation. **D** and **I** further furnish the desired products **2a** and **3a** by *in situ* hydrolyzation, respectively. Concomitantly, the active catalysts are regenerated for the next catalytic cycle.

Conclusions

We have developed a highly regioselective *peri*- and *ortho*-C–H methylation of 1-naphthaldehyde by using the transient ligand strategy. Mechanistically, capture of reaction intermediates and isotopic exchange experiments identified variable reactive metallacycles formed with different transient directing ligands in the metal-insertion and methylation steps. As suggested by DFT calculations and IBO analysis, although *peri*-metalation is energetically favorable compared to *ortho*-metalation in both palladium and iridium catalyses, transmetallation of CH_3BF_3K with iridium(III) readily takes place on the *ortho*-iridacycle rather than on the *peri*-iridacycle, which primarily explained the dichotomic selectivity on the two proximal positions of the naphthalene ring. We believe that this finding would greatly advance the future studies toward exquisite transformation control of polyaromatic rings. Moreover, the regioselectivity and broad utility of this method provide an unconventional tactic for the supply of multi-substituted naphthalene-based bioactive derivatives and natural products, thus building a stage for the use of dual metal/TDG catalysis approaches in the creation of molecules that are synthetically practicable and structurally attractive.

Data availability

All the experimental data have been included in the ESI.†

Author contributions

Y. M., J. J. and Y. Z. conceived and designed the project. Y. M., J. J. and D. Y. performed the experiments and collected the data. D. Y. and Y. M. contributed to the theoretical and experimental mechanistic investigation. X. C. and Y. W. contributed to the optimization of the transient directing strategy and the interpretation of the related results. Y. M., L. H. and Y. Z. prepared the manuscript with input from all contributing authors.

Conflicts of interest

There are no conflicts to declare.

Acknowledgements

This work was supported by the National Natural Science Foundation of China (No. 21877062, YZ), the "ShuangChuang" research team of Jiangsu Province (No. 20182036, YZ and LH), and the "Innovative and Entrepreneurial Talent" program (LH). We thank Prof. Donghui Wang for his constructive suggestion in the KIE study.

Notes and references

1 (*a*) E. J. Barreiro, A. E. Kümmerle and C. A. M. Fraga, *Chem. Rev.*, 2011, **111**, 5215–5246; (*b*) H. Schönherr and T. Cernak, *Angew. Chem., Int. Ed.*, 2013, **52**, 12256–12267.
2 G. Yan, A. J. Borah, L. Wang and M. Yang, *Adv. Synth. Catal.*, 2015, **357**, 1333–1350.
3 (*a*) E. Gwilherm and T. Cédric, *Angew. Chem., Int. Ed.*, 2019, **58**, 7202–7236; (*b*) S. D. Friis, M. J. Johansson and L. Ackermann, *Nat. Chem.*, 2020, **12**, 511–519.
4 (*a*) S. Okumura, S. Tang, T. Saito, K. Semba, S. Sakaki and Y. Nakao, *J. Am. Chem. Soc.*, 2016, **138**, 14699–14704; (*b*) S. Liang, M. Bolte and G. Manolikakes, *Chem.–Eur. J.*, 2017, **23**, 96–100; (*c*) J. Li, Y. Wang, Y. Yu, R. Wu, J. Weng and G. Lu, *ACS Catal.*, 2017, **7**, 2661–2667; (*d*) C. Jing, X. Chen, K. Sun, Y. Yang, T. Chen, Y. Liu, L. Qu, Y. Zhao and B. Yu, *Org. Lett.*, 2019, **21**, 486–489; (*e*) M. Zhang, A. Luo, Y. Shi, R. Su, Y. Yang and J. You, *ACS Catal.*, 2019, **9**, 11802–

11807; (*f*) S. Prévost, *ChemPlusChem*, 2020, **85**, 476–486; (*g*) B. Large and D. Prim, *Synthesis*, 2020, **52**, 2600–2612.

5 Examples of picolinamide directed C8–H founctionalization of naphthalene, see: (*a*) L. Huang, Q. Li, C. Wang and C. Qi, *J. Org. Chem.*, 2013, **78**, 3030–3038; (*b*) E. T. Nadres, G. I. F. Santos, D. Shabashov and O. Daugulis, *J. Org. Chem.*, 2013, **78**, 9689–9714; (*c*) R. Odani, K. Hirano, T. Satoh and M. Miura, *J. Org. Chem.*, 2013, **78**, 11045–11052; (*d*) L. Huang, X. Sun, Q. Li and C. Qi, *J. Org. Chem.*, 2014, **79**, 6720–6725; (*e*) R. Shang, L. Ilies and E. Nakamura, *J. Am. Chem. Soc.*, 2015, **137**, 7660–7663; (*f*) Z. Li, S. Sun, H. Qiao, F. Yang, Y. Zhu, J. Kang, Y. Wu and Y. Wu, *Org. Lett.*, 2016, **18**, 4594–4597; (*g*) Y. Xiong, Y. Yu, J. Weng and G. Lu, *Org. Chem. Front.*, 2018, **5**, 982–989; (*h*) S. Rej and N. Chatani, *ACS Catal.*, 2018, **8**, 6699–6706; (*i*) T. Zhang, H. Zhu, F. Yang, Y. Wu and Y. Wu, *Tetrahedron*, 2019, **75**, 1541–1547; (*j*) X. Yu, F. Yang, Y. Wu and Y. Wu, *Org. Lett.*, 2019, **21**, 1726–1729; (*k*) Y. Yao, Q. Lin, W. Yang, W. Yang, F. Gu, W. Guo and D. Yang, *Chem.–Eur. J.*, 2020, **26**, 5607–5610; (*l*) C. Zu, T. Zhang, F. Yang, Y. Wu and Y. Wu, *J. Org. Chem.*, 2020, **85**, 12777–12784.

6 (*a*) M. Shigeno, Y. Nishii, T. Satoh and M. Miura, *Asian J. Org. Chem.*, 2018, **7**, 1334–1337; (*b*) S. Moon, Y. Nishii and M. Miura, *Org. Lett.*, 2018, **21**, 233–236; (*c*) K. Yan, M. Liu, J. Wen, S. Wang, J. Li and H. Wang, *Org. Lett.*, 2020, **22**, 7825–7830.

7 (*a*) J. Karthikeyan and N. Yoshikai, *Org. Lett.*, 2014, **16**, 4224–4227; (*b*) S. Warratz, C. Kornhaaß, A. Cajaraville, B. Niepötter, D. Stalke and L. Ackermann, *Angew. Chem., Int. Ed.*, 2015, **54**, 5513–5517; (*c*) A. Biafora, T. Krause, D. Hackenberger, F. Belitz and L. J. Gooßen, *Angew. Chem., Int. Ed.*, 2016, **55**, 14752–14755; (*d*) S. Li, G. Deng, F. Yin, C. Li and H. Gong, *Org. Chem. Front.*, 2017, **4**, 417–420; (*e*) G. Tan, Q. You and J. You, *ACS Catal.*, 2018, **8**, 8709–8714; (*f*) J. Garrec, M. Cordier, G. Frison and S. Prévost, *Chem.–Eur. J.*, 2019, **25**, 14441–14446.

8 (*a*) R. Shi, L. Lu, H. Xie, J. Yan, T. Xu, H. Zhang, X. Qi, Y. Lan and A. Lei, *Chem. Commun.*, 2016, **52**, 13307–13310; (*b*) S. Rej and N. Chatani, *Chem.–Eur. J.*, 2020, **26**, 11093–11098.

9 B. Su and J. F. Hartwig, *Angew. Chem., Int. Ed.*, 2018, **57**, 10163–10167.

10 X. Zhang, W. Si, M. Bao, N. Asao, Y. Yamamoto and T. Jin, *Org. Lett.*, 2014, **16**, 4830–4833.

11 (*a*) M. Iwasaki, M. Iyanaga, Y. Tsuchiya, Y. Nishimura, W. Li, Z. Li and Y. Nishihara, *Chem.–Eur. J.*, 2014, **20**, 2459–2462; (*b*) M. Kondrashov, S. Raman and O. F. Wendt, *Chem. Commun.*, 2015, **51**, 911–913.

12 X. Luo, J. Yuan, C. Yue, Z. Zhang, J. Chen, G. Yu and C. Che, *Org. Lett.*, 2018, **20**, 1810–1814.

13 (*a*) Y. Nishinaka, T. Satoh, M. Miura, H. Morisaka, M. Nomura, H. Matsui and C. Yamaguchi, *Bull. Chem. Soc. Jpn.*, 2001, **74**, 1727–1735; (*b*) X. Li, X. Gong, M. Zhao, G. Song, J. Deng and X. Li, *Org. Lett.*, 2011, **13**, 5808–5811.

14 Examples of TDG strategy, see: (*a*) Y. Wu, Y. Chen, T. Liu, M. D. Eastgate and J. Yu, *J. Am. Chem. Soc.*, 2016, **138**, 14554–14557; (*b*) F. L. Zhang, K. Hong, T. J. Li, H. Park and J. Q. Yu, *Science*, 2016, **351**, 252–256; (*c*) X. Liu, H. Park, J. Hu, Y. Hu, Q. Zhang, B. Wang, B. Sun, K. Yeung, F. Zhang and J. Yu, *J. Am. Chem. Soc.*, 2017, **139**, 888–896; (*d*) X. Chen, S. Ozturk and E. J. Sorensen, *Org. Lett.*, 2017, **19**, 6280–6283; (*e*) Y. Chen, Z. Wang, Y. Wu, S. R. Wisniewski, J. X. Qiao, W. R. Ewing, M. D. Eastgate and J. Yu, *J. Am. Chem. Soc.*, 2018, **140**, 17884–17894; (*f*) H. Park, P. Verma, K. Hong and J. Yu, *Nat. Chem.*, 2018, **10**, 755–762; (*g*) T. Bhattacharya, S. Pimparkar and D. Maiti, *RSC Adv.*, 2018, **8**, 19456–19464; (*h*) F. Li, Y. Zhou, H. Yang, Z. Wang, Q. Yu and F. Zhang, *Org. Lett.*, 2019, **21**, 3692–3695; (*i*) Y. Chen, Y. Wu, Z. Wang, J. X. Qiao and J. Yu, *ACS Catal.*, 2020, **10**, 5657–5662; (*j*) M. Ding, W. Hua, M. Liu and F. Zhang, *Org. Lett.*, 2020, **22**, 7419–7423; (*k*) G. Li, Q. Liu, L. Vasamsetty, W. Guo and J. Wang, *Angew. Chem., Int. Ed.*, 2020, **59**, 3475–3479; (*l*) N. Goswami, T. Bhattacharya and D. Maiti, *Nat. Rev. Chem.*, 2021, **5**, 646–659; (*m*) S. Bag, S. Jana, S. Pradhan, S. Bhowmick, N. Goswami, S. K. Sinha and D. Maiti, *Nat. Commun.*, 2021, **12**, 1393–1400; (*n*) N. Thrimurtulu, A. Dey, K. Pal, D. Maiti and C. M. R. Volla, *Adv. Synth. Catal.*, 2019, **361**, 1441–1446.

15 J. Jiang, D. Yuan, C. Ma, W. Song, Y. Lin, L. Hu and Y. Zhang, *Org. Lett.*, 2021, **23**, 279–284.

16 X. Chen and E. J. Sorensen, *J. Am. Chem. Soc.*, 2018, **140**, 2789–2792.

17 (*a*) X. Chen, J. Li, X. Hao, C. E. Goodhue and J. Yu, *J. Am. Chem. Soc.*, 2006, **128**, 78–79; (*b*) X. Chen, C. E. Goodhue and J. Yu, *J. Am. Chem. Soc.*, 2006, **128**, 12634–12635.

18 G. Xia, J. Weng, L. Liu, P. Verma, Z. Li and J. Yu, *Nat. Chem.*, 2019, **11**, 571–577.

19 (*a*) X. Chen and E. J. Sorensen, *Chem. Sci.*, 2018, **9**, 8951–8956; (*b*) A. Woźniak, J. Tan, Q. Nguyen, A. Madron Du Vigné, V. Smal, Y. Cao and N. Cramer, *Chem. Rev.*, 2020, **120**, 10516–10543.

20 (*a*) E. A. Doisy, S. B. Binkleya and S. A. Thayer, *Chem. Rev.*, 1941, **28**, 477–517; (*b*) J. S. Albert, C. Ohnmacht, P. R. Bernstein, W. L. Rumsey, D. Aharony, Y. Alelyunas, D. J. Russell, W. Potts, S. A. Sherwood, L. Shen, R. F. Dedinas, W. E. Palmer and K. Russell, *J. Med. Chem.*, 2004, **47**, 519–529; (*c*) D. Heckmann, A. Meyer, B. Laufer, G. Zahn, R. Stragies and H. Kessler, *ChemBioChem*, 2008, **9**, 1397–1407; (*d*) P. Kasaplar, Ö. Yılmazer and A. Çağır, *Bioorg. Med. Chem.*, 2009, **17**, 311–318; (*e*) M. Al Kobaisi, S. V. Bhosale, K. Latham, A. M. Raynor and S. V. Bhosale, *Chem. Rev.*, 2016, **116**, 11685–11796; (*f*) T. Liu, H. Wu, J. Zhang, W. Deng and L. Yang, *J. Nat. Prod.*, 2020, **83**, 185–193.

21 P. Torres, R. Chinchilla, M. C. Asensi and M. Grande, *Phytochemistry*, 1989, **28**, 3093–3095.

22 Y. Hirai, M. Doe, T. Kinoshita and Y. Morimoto, *Chem. Lett.*, 2004, **33**, 136–137.

23 M. Braasch-Turi and D. C. Crans, *Molecules*, 2020, **25**, 4477–4513.

24 G. Knizia and J. E. M. N. Klein, *Angew. Chem., Int. Ed.*, 2015, **54**, 5518–5522.

25 D. L. Davies, S. A. Macgregor and C. L. McMullin, *Chem. Rev.*, 2017, **117**, 8649–8709.

26 K. Shin, Y. Park, M. Baik and S. Chang, *Nat. Chem.*, 2018, **10**, 218–224.